Realizable higher-dimensional two-particle entanglements via multiport beam splitters

Marek Żukowski,[1,2] Anton Zeilinger,[1] and Michael A. Horne[1,3]
[1]*Institut für Experimentalphysik, Universität Innsbruck, A-6020 Innsbruck, Austria*
[2]*Instytut Fizyki Teoretycznej i Astrofizyki, Uniwersytet Gdański, PL-80-952 Gdańsk, Poland*
[3]*Stonehill College, North Easton, Massachusetts 02357*
(Received 29 July 1996)

Multiport beam splitters are shown to be applicable in feasible optical realizations of higher-dimensional EPR correlations, and of tests of local realism involving measurements of nondichotomic variables. These multiports permit optical realizations of any unitary operator in Hilbert spaces of arbitrary finite dimension. Thus it is shown that one is by no means constrained to entangled spin systems, and to Stern-Gerlach apparatuses. In the analysis the concept of generalized Bell numbers is employed, which is more suitable than the standard set of spin eigenvalues. The results presented here move the discussion on entangled higher-than-$\frac{1}{2}$ spin systems from the realm of gedanken experiments to real experiments. [S1050-2947(97)07802-5]

PACS number(s): 03.65.Bz, 42.50.Dv, 89.70.+c

I. INTRODUCTION

Two problems connected with the notion of quantum entanglement (Schrödinger, 1935 [1]) and its consequences in the form of the Bell theorem are studied here. These are (a) a search for additional tests against local realism, and (b) attempts to extend the Bell theorem to nonstandard phenomena and to find forms for it. Both aspects are intertwined, as a theoretical analysis of the consequences of these other experiments often requires different versions of Bell's inequalities.

So far, no one can claim empirical falsification of the most general premises of local realism. The widespread opinion that the delayed-choice polarization-correlation experiments of Aspect, Dalibard, and Roger [2] constitute a once-and-for-all falsification of the local realistic position assumes that the experiments were closer to ideal than was actually the case. These experiments, as well as the multitude of other ones, from the first one by Freedman and Clauser (1972) [3] to the most recent ones (e.g., Tapster, Rarity, and Owens [4]), only refute various classes of local-realistic theories which additionally incorporate a version of the fair sampling assumption. They constitute a strong support for anyone also expecting violations of Bell's inequalities in (future) high collection efficiency experiments. Yet, even if one expects quantum mechanics to be finally definitively confirmed, as the present authors do, one has to admit that local realistic explanations of existing experiments are still not completely ruled out [5]. The evidence is not fully compelling, and, as physics is an experimental science, there is an obvious need for actually performing further experiments.

The new experiments could be reruns of the old ones with much better equipment (especially detectors) and more reliable sources. However, widening the palette of phenomena, and ranges of parameters, configurations, etc. available for an experimenter deciding to seek the most efficient way to close some, if not all, loopholes seems to be an important task (see, e.g., the reviews by Clauser and Shimony [6], Ballentine [7], Greenberger *et al.* [8], Home and Selleri [9], Belinskii and Klyshko [10], and Peres [11]).

It is important to show that experimentally accessible Einstein-Podolsky-Rosen (EPR) Bell phenomena are not limited solely to spin or polarization correlations [12]. Currently we are witnessing the emergence of interesting methods of producing entangled states. Cascade sources [2,3] have already been replaced be parametric down-conversion [13,14]. Atomic interferometry and micromaser techniques have also been proposed for production of Greenberger-Horne-Zeilinger (GHZ) three-particle entanglement [15,16]. Exciting applications have been found for EPR phenomena. The most spectacular of these seem to be quantum cryptography [17], quantum teleportation [18], and ''four-way'' coding on a single photon [19]. The techniques developed in the process can be applied for the study of other phenomena like ''superluminal'' tunneling [20] or nonclassical behavior of light [21]. A branch of EPR phenomena involving independent sources of particles is emerging [22,23].

The present work is devoted to some nonstandard methods of obtaining entangled photons. The possibility of performing a Bell-type experiment for nondichotomic observables is discussed. Such experiments differ from the conventional ones in many respects. First of all a Hilbert space of three or more dimensions describes the possible states of each of the subsystems (here a photon). Thus the theorem of Gleason [24], and the later ones of Bell [25] and Kochen and Specker [26] on noncontextual hidden variable theories, can be applied. Any realistic theory that would attribute a definitive result for each individual member of the ensemble described by a quantum-mechanical state, and would reproduce the quantum predictions, must be inevitably contextual. That is, the result of a single act of measurement of a certain observable must be dependent on its context (that is, whether we measure the observable alone or together with a different one, etc.). The original Bell theorem is formulated for two (entangled) two-dimensional subsystems, for each of which such problems do not arise. For an individual subsystem described in two-dimensional Hilbert space, one can always construct a noncontextual ''cryptodeterministic'' model. The contradiction with local reality emerges only when one considers correlations between two or more particles. In short, for higher dimensional cases, realistic descriptions already face conceptual problems at the level of a single subsystem.

This has an interesting consequence in the form of the argument of Heywood and Redhead [27]. By exploiting the perfect EPR correlations, which are characteristic of the singlet (entangled) state of two spins 1, they showed that even *local and locally contextual* deterministic hidden variable theories of such a system are incompatible with quantum mechanics. Their condition of local contextuality was introduced to avoid the Kochen-Specker contradiction for a single spin. But the EPR correlations in effect introduce *elements of reality*, and noncontextuality again arises. Thus the Kochen-Specker reasoning is applicable again.

Despite these interesting features of higher-dimensional systems, they are not in the mainstream of the research on the foundations of quantum physics. Most probably this is due to the complete lack of experimental results. The theoretical research on ''higher spin EPR-Bell correlations;'' see, e.g., [11] and [28], focuses on the spin-correlated subsystems extending the spin to arbitrarily high values. This is mainly motivated by the intention of verifying the very common belief that classical properties emerge in the limit of large quantum numbers (the actual results of the investigations suggest a far more ambiguous situation). However, so far no experiment, even for unit spins, has been performed, to our knowledge. This is due mainly to the lack of easily controllable sources emitting pairs of spin-1 (or higher) entangled objects [29].

This situation can be changed in two ways. First of all, optical experiments of the EPR-Bell type involving correlations of nondichotomic variables can indeed be performed: the phenomenon of spontaneous parametric down-conversion can be used to obtain an optical analog of the singlet state for two correlated spins (of arbitrary magnitude) [30], this two-photon state can be fed into certain aggregates of optical devices (which we shall call multiport beam splitters). As a result, higher-dimensional EPR-Bell correlations should be observed [30]. A version of the Bell theorem can be formulated for the predicted two-photon interference phenomena.

One can design exact optical analogs of the Stern-Gerlach apparata. However, the imagination should not be restricted to finding some photonic equivalents of such devices only. One can, e.g., try to generalize the optical nonpolarization test of the Bell inequalities to the case of nondichotomic local measurements. In this context, here we discuss optical devices [30] which we shall call symmetric Bell multiports. These multiport beam splitters enable one to obtain an additional class of possible EPR-Bell experiments (involving correlations of systems effectively described by Hilbert spaces of dimension higher than two).

Surprisingly, due to some historical peculiarity of the evolution of the theoretical research in the field almost the entire effort was so far limited to spin-correlated systems. As, in our case, we no longer deal with spins, it clear that a nonstandard method of value assignment can be introduced (by what we mean representation of a given result, i.e., a ''click'' at certain detector, by a number). It is argued that the use of suitably chosen complex numbers of unit modulus (roots of unity) is more convenient than the standard sets of spin eigenvalues. This is one more departure from the standard treatments.

The experiments with multiport beam splitters presented here seem to be the first feasible proposal for nondichotomic Bell tests. Six-port and eight-port beam splitters have already been constructed and tested in the laboratory [30]. Some statistical quantum effects that can be predicted for multiport beam splitters were tested. To this end a six-port and, in a separate experiment, an eight-port beam splitter were fed with the two-photon radiation of a parametric down-converter. Highly nonclassical counting statistics were observed. EPR-Bell experiments involving six-port beam splitters are underway [32].

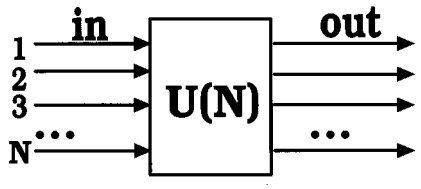

FIG. 1. A general U(N) beam splitter: an optical device capable of reproducing all N-dimensional unitary transformations.

Multiport beam splitters

Certain aggregates of simpler optical devices can be treated as multiport beam splitters [30]. The idea of a multiport beam splitter was discussed in Ref. [33] for the specific case of homodyne detection schemes. The application of multiport beam splitters in the context of Bell's theorem was suggested by Klyshko [34]. He briefly discussed the specific case of a six-port device, as a potential method of generalizing earlier experiments, without giving any predictions of the EPR correlations, or other phenomena to be expected for such systems.

As it was shown in [35], multiport devices can reproduce all finite-dimensional unitary transformations (for single-photon states). Such devices can be constructed using solely the standard (two-input–two-output) beam splitters, mirrors, and phase shifters. This opens the way to build optical analogs of various measuring apparata (e.g., the Stern-Gerlach ones, to be discussed below).

We are interested in reversible unitary processes. Thus here we shall study only lossless multiports of N input ports and N output ports (some ports can work both as input and output ports, viz. the Michelson interferometer); see Fig. 1. The operation of such a device is described by a unitary matrix U_N which gives the probability amplitudes for a single particle (photon) entering via input i to leave the device by output j (the subscript denotes the dimension of the matrix). If we assume monochromatic radiation in each of the beams, then we can represent the input beams by simple kets $|i\rangle$ and the output ones by $|j\rangle$, and the elements of U_N are given by

$$U_{Nji}=\langle j|U_N|i\rangle. \tag{1}$$

Within such a description the multiport device is treated as a passive linear mode coupler. The assumption of strict monochromaticity enables us to skip all considerations concerning the lengths of various optical paths within the studied devices. However, it will be evident (see the figures) that for the multiports presented here this aspect essentially poses no problems.

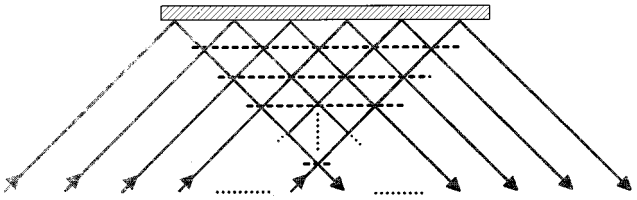

FIG. 2. A specific pyramidlike construction of a U(N) beam splitter.

The specific construction used by Reck *et al.* [34] is based on an earlier proposal [30] to use a pyramidlike network of standard beam splitters (i.e., of two input and two output ports), mirrors and phase shifters (for details, see Fig. 2). Here we shall try to present a straightforward *physical* reasoning which may replace the mathematical proof of [34]. Imagine (Fig. 3) a single photon entering, via the input port which we call N, a sequence of $N-1$ standard 2×2 beam splitters. The sequence is built in such a way that one output beam of the kth beam splitter (for $k<N-1$) is fed into the input port of the next beam splitter. It is obvious that one can always select the values of reflectivities and transmittivities for each beam splitter in such a way that all the probabilities $p(i)$, $i=1,\ldots,N$ for the photon to leave by the exit port i can be made arbitrary (except for the obvious constraint of adding up to 1). Further, one is always free to put a phase shifter behind every exit port, 1 to $N-1$ (the Nth phase is irrelevant—only relative phases are observable). If we denote the phase shifts as $\phi(i)$, then the quantum-mechanical amplitude for the photon to leave by the i-th exit port must be $\sqrt{p(i)}e^{i\phi(i)}$. Of course, one can always select the probabilities and phases in such a way that

$$\langle N|U_N|i\rangle=\sqrt{p(i)}e^{i\phi(i)}. \tag{2}$$

Note that in the above reasoning we have tacitly assumed that action of all the 2×2 beam splitters upon the state of the photon is described by a unitary matrix of real coefficients, e.g., of the type

$$\begin{bmatrix} \sin\theta & \cos\theta \\ \cos\theta & -\sin\theta \end{bmatrix}. \tag{3}$$

Now imagine a single photon prepared in the state, which can be represented as

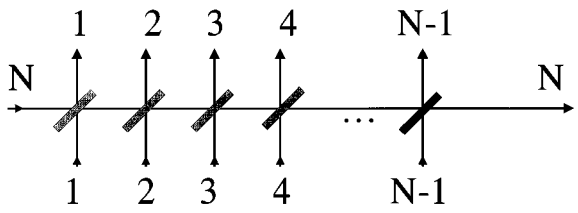

FIG. 3. A row of beam splitters which can produce any one-photon pure state (of the N-dimensional Hilbert space). The photon enters the system via the input N. The moduli of the amplitudes of the output state are determined by the reflectivities of the beam splitters. Suitable phase shifts behind the exits define the complex phase of the amplitude.

$$\begin{pmatrix} \sqrt{p(1)}e^{-i\phi(1)} \\ \cdot \\ \cdot \\ \sqrt{p(i)}e^{-i\phi(i)} \\ \cdot \\ \cdot \\ \sqrt{p(N)}e^{-i\phi(N)} \end{pmatrix}, \tag{4}$$

and then enters the beam-splitter sequence via the ports which were previously the output ports, but now work as the input ones. The unitary transformation, denoted as $T_{(N-1)}$, performed now by the multiport, will, of course, result in the photon leaving by the (now) output port N with probability 1. That is, the device operating in the reverse mode transforms the initial state represented by Eq. (4) into

$$(0,0,\ldots,0,1)^T. \tag{5}$$

Thus the Nth row [Eq. (2)] of the unitary matrix U_N can be transformed into Eq. (5). In other words, one has

$$T_{(N-1)}U_N=U_{(N-1)}\otimes I_N, \tag{6}$$

where $U_{(N-1)}$ is a unitary matrix acting in the $N-1$ dimensional subspace of the full Hilbert space (describing the, now output, modes 1 to $N-1$), and I_N is the identity operator acting in the last dimension (i.e., the Nth propagation mode).

Thus the problem of reproducing the matrix U_N by the devices described by Eq. (1) has been therefore reduced by one dimension. After $N-1$ steps like Eq. (6) we reduce the matrix to

$$\bigotimes_{i=1}^{N} I_i. \tag{7}$$

Thus, in this way, we constructed a pyramidlike device which imparts on the photon the unitary transformation U_N^{-1}. This ends our proof. For further details concerning this construction please consult [35].

II. SYMMETRIC MULTIPORT BEAM SPLITTERS IN EPR-BELL-TYPE EXPERIMENTS

All experimental work concerning the EPR-Bell correlations thus far was restricted to two-particle, mostly two-photon, entangled states, for which each subsystem could be effectively described by a two-dimensional Hilbert space (the first exception from this rule is the experiment, based on the ideas of the present paper, reported in [31]). The entangled spin-$\frac{1}{2}$ states were introduced by Bohm [36]. In the pioneering experiment by Freedman and Clauser [3], photon polarization entanglement was employed. While all work, with the exception of the original EPR paper, was restricted to entanglement of internal variables, in 1985 it was [12] proposed to use entanglement of external variables. Each of the photons could now be in one of the two distinctive beams; thus again one subsystem was effectively described by a two-dimensional Hilbert space. Bell-type local yes-no dichotomic measurements [37] could be now performed. The

local measuring apparata were proposed to consist of a 50-50 beam splitter, a phase shifter in front of it, and two photodetectors behind it (exactly such an experiment was performed by Rarity and Tapster [38] in 1990).

A natural extension of the scheme presented in [12] is to have two particles in an entangled state, with three or more, generally N possible beams for each particle. Having this, one can apply locally phase shifts in $N-1$ beams, and, farther downstream, feed these beams into a local N-input–N-output generalized beam splitter (to be called a $2N$ multiport here), and observe coincidences behind two spatially separated devices of this kind.

We shall consider here only *symmetric* multiport devices [29], which are defined such that the squared moduli of all their input-port–output-port transition amplitudes are equal to $1/N$. Such a system will perform a local unitary transformation on each of the entangled photons, which would finally end up in one of the N detectors behind an output port. The 50-50 beam splitter is the simplest member of the family. All such objects have the following physical property: if one photon enters into any single input port its chances of exit are equally split between all output ports.

We treat the multiport beam splitters as devices which perform a specified unitary transformation. Thus if we change any element of their construction in such a way that we obtain as a result a different transformation matrix we will treat this as a different device. However, if one excludes from the set of possible modifications (i) the trivial operations of supplying external phase shifters in front of the input ports and behind the output ones, and also (ii) mere relabelling of the output ports, one immediately obtains equivalence classes of multiports which can be transformed into each other with these external operations. From now on, in this section, we shall limit our study to only representative members of such classes. In all applications it is enough just to know the nontrivial properties of one member of such a class.

If one has a $N\times N$ unitary matrix representing a symmetric multiport beam splitter, it is always possible to absorb any phase factors of the first row into phases of the input beams, and to absorb the phase factors of the first column into phases of the output beams. After such manipulations the matrix representing the multiport, if one extracts the common modulus $\sqrt{1/N}$, contains only 1's in both the first column and the first row. Such a matrix is called real bordered [39]. Multiports endowed with such transformation matrices will be taken as the representatives of the equivalence classes defined earlier. Only such devices will be discussed in this section.

A. Standard beam splitter

The simplest symmetric multiport is a 50-50 beam splitter. It is very easy to show that all such devices form one equivalence class represented by the beam splitter of the following transformation matrix:

$$\sqrt{1/2}\begin{pmatrix} 1 & 1 \\ 1 & -1 \end{pmatrix}. \tag{8}$$

Thus if it operates in a two-dimensional Hilbert space, all the elements of the matrix are powers of $-1=\exp(i2\pi/2)$.

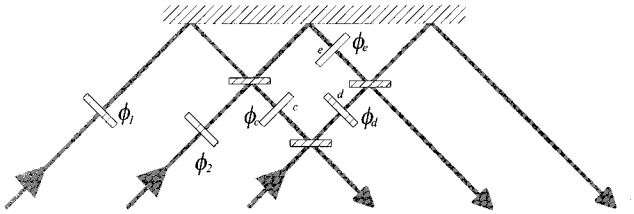

FIG. 4. Tritter. The lowermost beam splitter has a reflectivity $R=\frac{1}{3}$; for the other two $R=\frac{1}{2}$, and at the top we have a mirror, i.e., an $R=1$ device. If suitable internal phase shifts are applied, the probabilities for a single photon entering via any input port to exit via any output are equal.

B. Tritter

The *tritter* [30] is a generalization of the 50-50 beam splitter to systems described in three-dimensional Hilbert spaces. Unitarity, the requirement that all its elements are of the same modulus, and finally the real-bordered form of it, limit the tritter transition matrix to the following:

$$\sqrt{1/3}\begin{pmatrix} 1 & 1 & 1 \\ 1 & c & c^* \\ 1 & c^* & c \end{pmatrix}, \tag{9}$$

with $c=\exp(\pm i2\pi/3)$. Having at our disposal the possibility of relabelling the output ports, which is equivalent to permutation of the rows one can rewrite the tritter matrix as:

$$\sqrt{1/3}\begin{pmatrix} 1 & 1 & 1 \\ 1 & \alpha^1 & \alpha^2 \\ 1 & \alpha^2 & \alpha^4 \end{pmatrix}, \tag{10}$$

where

$$\alpha=\exp(i2\pi/3). \tag{11}$$

That is, all matrix elements are powers of α, and are given by

$$\mathbf{U}^3_{ij}=\alpha^{(i+j-2)}=\exp[(i2\pi/3)(i-1)(j-1)]. \tag{12}$$

Again we notice that all elements of a tritter are powers of the same root of unity $\exp(i2\pi/3)$. Further, just like in the case of the 50-50 beam splitter, there is only one tritter (i.e., one class of equivalence). This will not be so for devices of still higher dimensions. A specific optical design of a tritter is given in Fig. 4.

One can easily check that the device of Fig. 4 has the required properties. Assume that action of the 2×2 beam splitters of the configuration is described by the product:

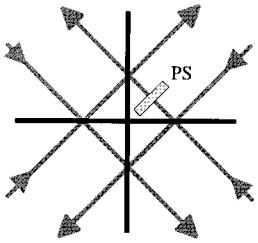

FIG. 5. Symmetric eight-port beam splitter. The phase ϕ of Eq. (12) can be fixed by a single-phase shifter PS inserted into one of the internal paths within the device. Each value of the phase defines equivalence class of symmetric eight-port beam splitters.

$$\begin{pmatrix} \frac{1}{\sqrt{2}} & i\frac{1}{\sqrt{2}} & 0 \\ i\frac{1}{\sqrt{2}} & \frac{1}{\sqrt{2}} & 0 \\ 0 & 0 & 1 \end{pmatrix} \begin{pmatrix} \sqrt{\frac{2}{3}} & 0 & i\frac{1}{\sqrt{3}} \\ 0 & 1 & 0 \\ i\frac{1}{\sqrt{3}} & 0 & \sqrt{\frac{2}{3}} \end{pmatrix} \times \begin{pmatrix} 1 & 0 & 0 \\ 0 & \frac{1}{\sqrt{2}} & i\frac{1}{\sqrt{2}} \\ 0 & i\frac{1}{\sqrt{2}} & \frac{1}{\sqrt{2}} \end{pmatrix}. \tag{13}$$

The three matrices upon multiplication give

$$\frac{1}{\sqrt{3}} \begin{pmatrix} 1 & i & i \\ e^{i2\pi/3} & e^{-i\pi/6} & i \\ e^{i5\pi/6} & e^{i2\pi/3} & 1 \end{pmatrix}, \tag{14}$$

i.e., the device is indeed a tritter. Please note that this specific construction does not require internal phase shifts.

C. Symmetric eight-port beam splitters

Turning to higher-multiport devices, one of the most interesting results is the existence of distinct equivalence classes. That is, the (real-bordered) transition matrices of symmetric eight-port beam splitters are given by [32]

$$2^{-1} \begin{pmatrix} 1 & 1 & 1 & 1 \\ 1 & e^{i\phi} & -1 & -e^{i\phi} \\ 1 & -1 & 1 & -1 \\ 1 & -e^{i\phi} & -1 & e^{i\phi} \end{pmatrix}. \tag{15}$$

Thus we have infinitely many nonequivalent eight-port devices, one for each choice of ϕ . The equivalence classes are (continuously) parametrized by the phase ϕ of the range between 0 and π. This phase is very transparent in the specific construction, tested in [30], of a symmetric eight-port device given in Fig. 5. However, different realizations are also possible; see Fig. 2. Please note that, if one sets $\phi=\pi/2$, the resulting multiport beam splitter has matrix elements which are again powers of a root of unity, this time $i=\exp(i2\pi/4)$.

The device of Fig. 5 does not have a pyramidlike structure. This construction requires fewer optical elements. To check that the device of Fig. 5 has the required properties, assume that action of the 2×2 beam splitters and the phase shifter of the configuration is described by the product

$$\begin{pmatrix} \frac{1}{\sqrt{2}} & 0 & \frac{1}{\sqrt{2}} & 0 \\ -\frac{1}{\sqrt{2}} & 0 & \frac{1}{\sqrt{2}} & 0 \\ 0 & \frac{1}{\sqrt{2}} & 0 & \frac{1}{\sqrt{2}} \\ 0 & -\frac{1}{\sqrt{2}} & 0 & \frac{1}{\sqrt{2}} \end{pmatrix} \begin{pmatrix} e^{i\phi} & 0 & 0 & 0 \\ 0 & 1 & 0 & 0 \\ 0 & 0 & 1 & 0 \\ 0 & 0 & 0 & 1 \end{pmatrix} \times \begin{pmatrix} \frac{1}{\sqrt{2}} & \frac{1}{\sqrt{2}} & 0 & 0 \\ -\frac{1}{\sqrt{2}} & \frac{1}{\sqrt{2}} & 0 & 0 \\ 0 & 0 & \frac{1}{\sqrt{2}} & \frac{1}{\sqrt{2}} \\ 0 & 0 & -\frac{1}{\sqrt{2}} & \frac{1}{\sqrt{2}} \end{pmatrix}. \tag{16}$$

The resulting unitary transformation reads

$$\frac{1}{2} \begin{pmatrix} e^{i\phi} & e^{i\phi} & 1 & 1 \\ -e^{i\phi} & -e^{i\phi} & 1 & 1 \\ -1 & 1 & -1 & 1 \\ 1 & -1 & -1 & 1 \end{pmatrix}, \tag{17}$$

i.e. the device is indeed a quarter.

D. Higher symmetric multiport beam splitters: Bell multiports

Higher-dimensional multiport beam splitters can be constructed using the procedure shown in Fig. 2. Here we shall discuss only the case of the higher symmetric multiports of certain specific properties. One can always build an $2N$ port with the distinguishing trait that the elements of its transition matrix, $\mathbf{U}^N$, are built *solely* out of powers of the Nth root of unity

$$\gamma_N=\exp(i2\pi/N), \tag{18}$$

namely,

$$\mathbf{U}^N_{ji}=\langle j'|\mathbf{U}^N|i\rangle=\frac{1}{\sqrt{N}}\gamma_N^{(j-1)(i-1)}. \tag{19}$$

Unitarity of $\mathbf{U}^N$ can be checked with the use of the following property of the roots of unity:

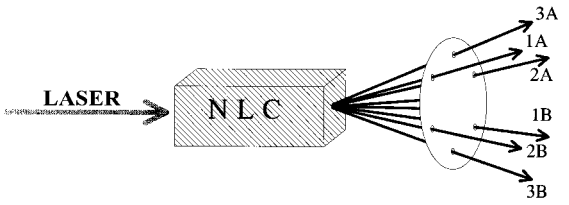

FIG. 6. The type-I spontaneous parametric down conversion process (PDC). Very strong monochromatic laser light shines upon a crystal endowed with a quadratic nonlinearity. Some pump photons spontaneously decay into pairs of lower-energy photons. The emissions are strongly correlated in direction. The pinhole arrangement presented here is suitable for a two-tritter Bell-type experiment (see next figures).

$$\sum_{l=1}^{N} \gamma_N^{(m-1)(l-1)} \gamma_N^{-(k-1)(l-1)} = N \delta_{mk} . \tag{20}$$

Of course, for $N=2,\ 3$, and 4, exactly such devices were discussed above. We propose to call devices endowed with the property (19) as *Bell multiports* beam splitters. As we shall see below such devices possess very interesting properties which lead to straightforward generalizations of Bell-EPR experiments to the realm of nondichotomic observables.

An extensive study of the properties of such devices can be found in [40]. The symmetric multiport devices are an operational realization of the concept of *mutually unbiased bases*; see, e.g., [41]. Such bases are ''as different as possible'' [11]. A photon which is in the basis state $|i\rangle$ has equal chances to leave the symmetric multiport by any exit port. It is also worth noting that the matrices $\mathbf{U}_{ji}^{N}$ perform a discrete Fourier transform on sequences of N complex numbers.

III. EPR-BELL CORRELATIONS WITH MULTIPORT BEAM SPLITTERS

A. Preparation of the initial states

After having now introduced multiport beam splitters as physical devices which can perform a unitary transformation, we now turn to the question of the appropriate source that would enable us to feed two multiport devices with a certain entangled state leading to EPR-Bell correlations. We shall show below that such a source exists: it is the spontaneous parametric down-conversion process (PDC). We shall present the appropriate source for a two-tritter experiment [30], and later give its generalization to higher dimensions.

One can find in the literature very detailed theoretical descriptions of the PDC process (see, e.g., [42,43]). Thus, we shall only give its essential traits (Fig. 6). If one shines a strong monochromatic laser beam on a suitably cut and oriented crystal endowed with a quadratic nonlinearity, some pump photons spontaneously fission into pairs of photons of lower frequency (for historical reasons called signal and idler). The crystal acts as an elastic scatterer, and thus the energy of the photon field is conserved in the process. Therefore, the frequencies of pump photon ω_p, signal ω_s, and idler ω_i, satisfy

$$\omega_p = \omega_s + \omega_i . \tag{21}$$

There is no other restriction on the frequency of the PDC photons. The emission is extremely broadband. However, the geometry of the process leads to constructive interference of the spontaneous emissions into the so called *phase-matched* directions only. The photonic wave vectors satisfy (within the crystal)

$$\mathbf{k}_p \approx \mathbf{k}_s + \mathbf{k}_i . \tag{22}$$

The emissions are therefore strongly correlated directionally. The sharpness of Eq. (22) grows with the size of the crystal, and of the laser beam waist. If the crystal is cut in such a way that the so called type-I phase-matching condition is satisfied, both PDC photons are of the same polarization (note that crystals with quadratic nonlinearities are always noncentrosymmetric, and thus birefringent). Due to the phase matching condition (22) (single) photons of the same frequency are emitted into cones centered at the pump beam. By picking photons from a specially chosen cone one can have PDC radiation with both photons of equal frequency $\frac{1}{2}\omega_p$. The selection can be done by a suitable pinhole arrangement in a diaphragm behind the crystal (such an arrangement is shown in Fig. 6). N pairs of pinholes can be pierced at points on a circle, drawn on the diaphragm, and centered about the pump beam. The pinholes of each pair should be bored at points symmetric with respect to the center of the circle. If the down-conversion photon passes through one of the pinholes, then the other photon will pass through the diametrically opposite pinhole. Since there are N pairs of diametrically opposite pinholes, the state of the photon pair will be a superposition of passage through the N pairs of pinholes [13].

Such a source arrangement for the case $N=3$ is shown in Fig. 6. The state describing the coherent superposition for the pair of photons to leave the aperture system with equal probability by either the pinholes 1_A and 1_B or 2_A and 2_B or finally 3_A and 3_B can be written down as

$$|\psi(3)\rangle = \sqrt{1/3} \sum_{m=1}^{3} |m,A\rangle |m,B\rangle, \tag{23}$$

where, e.g., $|m,A\rangle$ describes a particle going through the pinhole m_A. This state is formally equivalent to the one of two spin-1 particles in a singlet state (which, theoretically, will produce interesting three way correlations in two Stern-Gerlach apparatuses).

Generalizing this method to arbitrary N, one can produce entangled states of the form

$$|\psi(N)\rangle = \sqrt{1/N} \sum_{m=1}^{N} |m,A\rangle |m,B\rangle. \tag{24}$$

The scheme for realization of such a state is a straightforward development of the idea shown in Fig. 6 (more pinholes at phase-matched directions).

B. Two-tritter EPR-Bell experiment

Let us now imagine two spatially separated experimenters who perform the following measurements. Each of their measuring apparata consist of a set of three phase shifters just in front of a tritter, and three photon detectors (perfect,

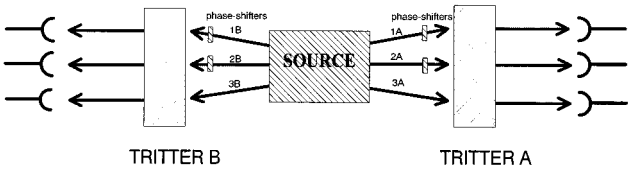

FIG. 7. A two-tritter Bell-type experiment. The two down-converted photons are fed into two (identical) spatially separated tritters. The phase shifters are placed close to the input ports of the tritters.

in the gedanken situation described here) which register photons in the output ports of the tritter (Fig. 7). The phase shifters serve the role of the devices which set the free macroscopic, classical parameters which can be controlled by the experimenters (just like the orientations of the Stern-Gerlach apparata, $\vec{a}$ and $\vec{b}$, for the original Bell's gedanken experiment). Please note that only two phase shifters on each side suffice (the phase is relative). Nevertheless, we shall retain three phase shifts for a while, as in this case the formulae have a very symmetric form, and their generalization to higher-dimensional case becomes obvious. The initial state is transformed by the phase shifters into

$$|\psi(3)'\rangle=\sqrt{1/3}\sum_{m=1}^{3}\exp[i(\phi_A^m+\phi_B^m)]|m,A\rangle|m,B\rangle, \quad (25)$$

where ϕ_A^m and ϕ_B^m describe the action of the phase shifters. The quantum prediction for the joint probability $P_{QM}(k,n)$ to detect a photon at the kth output of tritter A and another one at the nth output of B is given by:

$$P_{QM}(k,n)=\frac{1}{3}\left|\sum_{m=1}^{3}\exp[i(\phi_A^m+\phi_B^m)]\mathbf{U}_{mk}^3\mathbf{U}_{mn}^3\right|^2$$
$$=(1/3)^3\left|\sum_{m=1}^{3}\exp[i(\phi_A^m+\phi_B^m)]\alpha^{(m-1)(k+n)}\right|^2, \quad (26)$$

with, again, $\alpha=\exp i2\pi/3$. If one introduces $\Phi^{kn}\equiv\frac{2}{3}\pi(k+n-2)$, this can be put into the following form:

$$P_{QM}(k,n)=(1/3)^3\{3+2[\cos(\phi_A^1+\phi_B^1-\phi_A^2-\phi_B^2-\Phi^{kn})$$
$$+\cos(\phi_A^2+\phi_B^2-\phi_A^3-\phi_B^3-\Phi^{kn})$$
$$+\cos(\phi_A^3+\phi_B^3-\phi_A^1+\phi_B^1-\Phi^{kn})]\}. \quad (27)$$

Please note that

$$P_{QM}(1,1)=P_{QM}(2,3)=P_{QM}(3,2),$$
$$P_{QM}(1,2)=P_{QM}(2,1)=P_{QM}(3,3), \quad (28)$$
$$P_{QM}(1,3)=P_{QM}(2,2)=P_{QM}(3,1).$$

C. Two-tritter perfect EPR correlations

The perfect EPR correlations occur in the two tritter experiment when one of the probabilities has the value

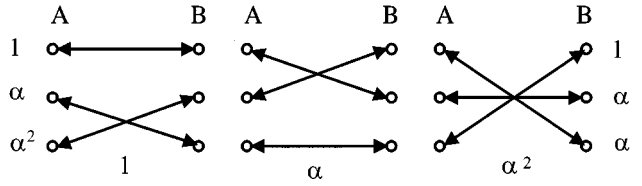

FIG. 8. EPR correlations for the two-tritter experiment. The first graph shows that for the specific settings of the local phases [Eq. (30)] firing of the uppermost detector behind the tritter A implies that the uppermost detector fires behind tritter B. When the middetector of A fires, one can predict with certainty the lowermost counter of B to fire, etc. The other two graphs are valid for settings (31) and (32), respectively. The value assignment procedure, which associates with each detector on one side a power of $\alpha=\exp(i2\pi/3)$, gives unique values for the products of such values for EPR-correlated detectors (as listed across the bottom).

$$P_{QM}(1,l)=\tfrac{1}{3}. \quad (29)$$

This implies that $P_{QM}(1,n)=0$, for all $n\neq l$. That is, all other joint probabilities vanish, except for the counts which satisfy $k+n=1+l$ (modulo 3). Thus when the phase shifts are set to the right values, a certain detector count at one spatially separated detector station implies with probability 1 firing of a specific detector on the other side. Thus we have a typical situation for which the Einstein-Podolsky-Rosen idea of elements of reality may be introduced. In the studied system such correlations arise for

$$\phi_A^1+\phi_B^1=\phi_A^2+\phi_B^2=\phi_A^3+\phi_B^3 \quad (30)$$

[$k+l=2$ (modulo 3) correlation] detection of a photon in $1_A'$ implies that another one will be detected in $1_B'$; detection at $2_A'$ implies a similar event at $3_B'$; and, finally, photon registration at $3_A'$ has to be accompanied by another one at $2_B'$. Similar situations occur for phase settings

$$\phi_A^1+\phi_B^1=\phi_A^2+\phi_B^2+2\pi/3=\phi_A^3+\phi_B^3+4\pi/3 \quad (31)$$

($k+l=3$ perfect correlations of $1_A'$ and $2_B'$, $2_A'$ and $1_B'$, 3_A and $3_B'$), and finally also for

$$\phi_A^1+\phi_B^1=\phi_A^2+\phi_B^2+4\pi/3=\phi_A^3+\phi_B^3+2\pi/3 \quad (32)$$

($k+l=1$ correlation: $1_A'$ with $3_B'$, $2_A'$ with $2_B'$, $3_A'$ with $1_B'$). Thus, while it is maximally uncertain which detector will register either of the particles, it is possible to predict with certainty which detector will register the second particle once the first particle is observed, as long as the phases are set according to one of the above three conditions. Figure 8 shows the three types of perfect correlations that arise from Eqs. (30), (31), and (32). [Note that there are actually six possible one-to-one combinations between three detectors on each side. The types of perfect correlations shown in Fig. 8 arise when we use the same tritter on each side. If we use a pair of tritters which differ by interchanging two outputs (in one of them), EPR correlations occur shown in Fig. 9, with the original three now being excluded.]

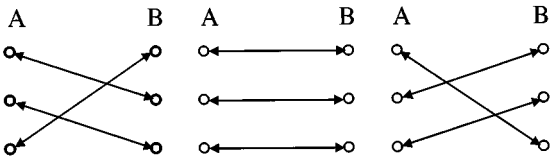

FIG. 9. The types of perfect correlations shown in Fig. 8 arise when we use the same tritter on each side. If we use a pair of tritters which differ by interchanging two outputs (in one of them), EPR correlations occur as shown above, with the original three now being excluded.

D. EPR correlations with two Bell multiport beam splitters

Here we shall discuss only the case of the EPR correlations in higher Bell multiport devices. The two spatially separated sets of phase shifters (one phase shifter in each beam) transform the initial state into

$$|\psi(N)'\rangle=\sqrt{1/N}\sum_{m=1}^{N}\exp[i(\phi_A^m+\phi_B^m)]|m,A\rangle|m,B\rangle, \tag{33}$$

where ϕ_A^m and ϕ_B^m, as before, denote the local phase shifts.

Each set of local phase shifts constitutes the interferometric realizations of the ''knobs'' at the disposal of the observer controlling the local measuring apparatus which incorporates also the Bell multiport device and N detectors. The quantum prediction for the joint probability $P^{(k,l)}$ to detect a photon at the kth output of the multiport A and another one at the lth output of the multiport B is given by

$$\begin{aligned}P_{QM}^{(k,l)}&=(1/N)\left|\sum_{m=1}^{N}\exp[i(\phi_A^m+\phi_B^m)]\mathbf{U}_{mk}^{N}\mathbf{U}_{ml}^{N}\right|^2\\&=(1/N^3)\left|\sum_{m=1}^{N}\exp[i(\phi_A^m+\phi_B^m)]\gamma_N^{(m-1)(k+l-2)}\right|^2,\end{aligned} \tag{34}$$

with γ_N given by Eq. (18). One can expand the square of the modulus, and this leads to

$$P_{QM}^{(k,l)}=\left(\frac{1}{N^3}\right)\left(N+2\sum_{m>n}^{N}\cos(\mathbf{\Phi}_{kl}^m-\mathbf{\Phi}_{kl}^n)\right), \tag{35}$$

where $\mathbf{\Phi}_{kl}^m\equiv\phi_A^m+\phi_B^m+[m(k+l-2)](2\pi/N)$. The counts at a single detector, of course, do not depend upon the local phase settings,

$$P_{QM}^{(k)}=P_{QM}^{(l)}=\frac{1}{N}. \tag{36}$$

The most important features of the quantum prediction are already visible in Eq. (34). The probability $P_{QM}(k,l)$ is dependent solely on the sum $k+l$ (modulo N, of course). The perfect correlations occur only when for certain l one has $P_{QM}(1,l)=1/N$ [again this implies that $P_{QM}(1,l')=0$ for all l' different from l]. Thus there are N classes of different perfect correlations. In each class correlated counts are expected only for outputs k (side A) and l (side B) for which $k+l$ has a specified fixed value (modulo N), no other events are allowed. Each detector on one side is allowed to fire only provided its unique partner fires on the other side. It is interesting to note that the N classes of allowed perfect correlations form a small subset of all the $N!$ members of the full set of one-to-one relations linking the detectors of side A with those of side B.

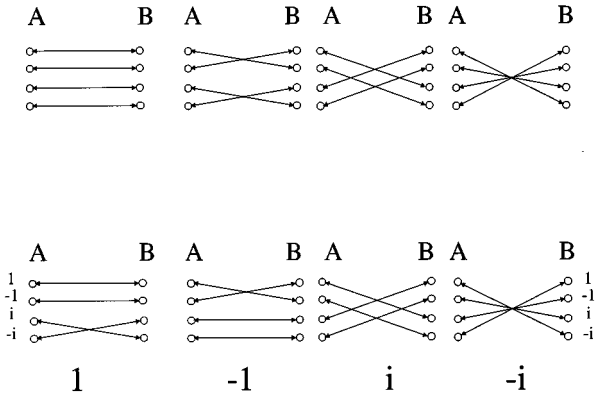

FIG. 10. EPR correlations for the experiment with two eight-port beam splitters. Compare the caption of the previous figure. The top row shows EPR correlations for two eight-port beam splitters, both with the internal phase setting at $\phi=0$ (thus they are not Bell multiports), whereas the bottom row is for phase settings $\phi=\pi/2$ (that is, for two identical Bell quarters). It is interesting that for the upper case the value assignment procedure, which associates with each detector on one side a power of $i=\exp(i2\pi/4)$, can *never* give unique values for the products of such values for EPR-correlated detectors. However, for $\phi=\pi/2$, the perfect EPR correlations shown in the bottom row have the property that the products of the values are unique, as listed across the bottom.

To illustrate further these features of the two Bell multiport device correlations, we present the full set of possible perfect EPR-correlations for an experiment with two eight-port beam splitters (Fig. 10). A four-member subset of all possible 4! graphs is realizable with a given pair of identical eight-port devices. One can trivially move to another set of graphs by a relabeling of the output ports.

IV. CORRELATION FUNCTIONS. NONCONVENTIONAL VALUE ASSIGNMENT: BELL NUMBERS

In his pioneering work, Bell [37] discussed the results of local measurements of dichotomic observables. The studied observables were the projections of spin-$\frac{1}{2}$ on certain directions (specified by the vector describing the orientation of the Stern-Gerlach apparatus). Motivated by simplicity, he renormalized the eigenvalues of the spin-$\frac{1}{2}$ operators to $+1$ and -1. The two numbers of Bell have the following properties: their sum is equal to 0, and they are the two square roots of unity. The correlation function of Bell [37] is defined as the average of the product of the two (local) dichotomic observables, and (for the singlet state) is given by

$$E(\vec{a},\vec{b})=-\vec{a}\cdot\vec{b}, \tag{37}$$

where the unit vectors specify the orientations of the two apparata. The perfect EPR correlations for the system considered by Bell occur for the parameter settings for which this correlation function is either equal 1 or -1. Thus the

two numbers, ± 1, naturally signify the two types of perfect correlations which are possible for the two spin-$\frac{1}{2}$ case. For a given perfect EPR correlation the product of the measured values of the two dichotomic variables always has the same value (± 1). We shall show below that for the two-Bell-multiport device experiment one can find a set of numbers with similar properties. One can associate them with photon registration acts at specified detectors. Surprisingly, these are not the numbers which form the usual set of eigenvalues of higher than $\frac{1}{2}$ spin projection operators.

Let us first discuss the two-tritter case. One might be tempted to assign the values $+1$, 0, and -1 to the three possible outcomes on each side. However, such a procedure has some disadvantages, because when calculating the product of the values (the way Bell did it), the appearance of a ''0'' result on any side always leads to a 0 value for the product, independent of which type of correlation occurs and thus information is lost. Therefore, here we propose a different procedure which aims at curing this problem. We assign the numbers α, α^2, and $\alpha^3=1$ to the three possible outcomes on either side. It then follows that the product of the two local values for the three cases of perfect EPR correlations are equal to powers of α (see Fig. 8). Our nonstandard choice can be expressed in the simplest way as the assignment of a value α^{k-1} to a detection event at the kth detector on a side. The usual features of the third complex roots of unity

$$\sum_{k=1}^{3} \alpha^k = 0, \qquad |\alpha^k| = 1 \tag{38}$$

are evident generalizations of the properties of the original Bell numbers.

The correlation function of Bell for our experiment defined with the use of these numbers reads

$$E(\phi_A^1, \phi_A^2, \phi_A^3; \phi_B^1, \phi_B^2, \phi_B^3) \tag{39}$$

$$= \sum_{k=1,\ l=1}^{3} \alpha^{(k-1)} \alpha^{(l-1)} P^{(k,l)}(\phi_A^1, \phi_A^2, \phi_A^3; \phi_B^1, \phi_B^2, \phi_B^3), \tag{40}$$

where $P^{(k,l)}$ is the probability of the firing of detectors k and l. For the perfect EPR correlations it acquires the value equal to one of the Bell numbers (that this is indeed so will be shown later).

Let us move to the general case of two $2N$ multiport devices. For the case of correlations between two particles fed into two spatially separated multiports, it is quite natural to try to generalize the procedure just given. However, we should point out, for $N>3$ this procedure, including the unconventional Bell values assignment of the Nth roots of unity to the detectors, seems to fail unless the multiport devices are Bell multiport devices [30] (see the caption of Fig. 9).

For the two-Bell-multiport device experiment (the one described in Sec. III) a good choice is to assign the value γ_N^{k-1} to a detection event at output k (the same assignment for both sides). The features of Nth complex roots of unity

$$\sum_{k=1}^{N} \gamma_N^k = 0, \qquad |\gamma_N^{(k-1)}| = 1 \tag{41}$$

are generalizations of the properties discussed earlier.

The generalized Bell correlation function should give the average value of the product of pairs results; thus in our case it reads

$$E(\phi_A^1, \ldots, \phi_A^N; \phi_B^1, \ldots, \phi_B^N) = \sum_{k=1}^{N} \sum_{l=1}^{N} \gamma_N^{k-1} \gamma_N^{l-1} P^{(k,l)}. \tag{42}$$

The quantum-mechanical prediction for this correlation function can be easily calculated in the following way. First we observe that

$$\sum_{k+l=m+1} \gamma_N^{k-1} \gamma_N^{l-1} P_{QM}^{(k,l)} = N \gamma_N^{m-1} P_{QM}^{(1,m)}, \tag{43}$$

and thus with the use of the explicit formula for the probabilities the overall expression for the correlation function becomes

$$\frac{1}{N^2} \sum_{l=1}^{N} \gamma_N^{l-1} \left| \sum_{m=1}^{N} \gamma_N^{(m-1)(l-1)} \exp[i(\phi_A^m + \phi_B^m)] \right|^2. \tag{44}$$

Now one can write the squared modulus as a product of a sum and its complex conjugate, and with the use of identity (20), one obtains

$$E(\phi_A^1, \ldots, \phi_A^N; \phi_B^1, \ldots, \phi_B^N) = \frac{1}{N} \sum_{m=1}^{N} \exp[i(\phi_A^m + \phi_B^m - \phi_A^{m+1} - \phi_B^{m+1})], \tag{45}$$

where the numerical values of the indices are to be understood modulo N. For $N=2$, it is easy to see that the function reduces to

$$\cos[(\phi_A^1 - \phi_A^2) + (\phi_B^1 - \phi_B^2)], \tag{46}$$

i.e., it acquires its standard form.

V. BELL THEOREM FOR THE MULTIPORT EXPERIMENTS

The quantum prediction for the joint probability $P_{QM}^{(k,l)}$ to detect a photon at the kth output of multiport A and another one at the lth output of B is given by Eq. (35) (we assume perfect detection and perfect interferometers), whereas the counts at a single detector, of course, do not depend upon the local phase settings (36). The predicted results of the experiments described above cannot be reproduced by any local realistic theory. We shall show below that this claim can be substantiated by the application of the Clauser-Horne Bell-inequalities (see, e.g., [6]).

Despite the fact that these inequalities were derived for the case of an experiment involving dichotomic variables, they are also useful for the two-Bell-multiport experiment, as we shall see. The Clauser-Horne (CH) inequalities impose constraints on coincident counts and singles counts at a cer-

tain pair of detectors. There is nothing in their original derivation which specifies what kind of quantum process is being monitored by the detector pair. Thus they are applicable to the counts at any pair of (spatially separated) detectors behind our multiport devices. Using our earlier notation, they can be put into the following form:

$$-1\leqslant P_{\mathrm{LR}}^{(k,l)}(a,b)+P_{\mathrm{LR}}^{(k,l)}(a,b')+P_{\mathrm{LR}}^{(k,l)}(a',b) - P_{\mathrm{LR}}^{(k,l)}(a',b')-P_{\mathrm{LR}}^{(k)}(a)-P_{\mathrm{LR}}^{(l)}(a)\leqslant 0, \quad (47)$$

where the letters LR indicate that the inequality is satisfied by theories that comply with the premises of *local realism*. The symbols a, a' and b, b' denote the settings of the local operational parameters, in our case the phase shifts ϕ_A^m, $\phi_A'^m$ and ϕ_B^m, $\phi_B'^m$ $(m=1,\ldots,N)$, i.e., $a=\{\phi^m;m=1,\ldots,N\}$, etc. The hidden variable version of a local realistic theory of the family of experiments introduced above requires that the probabilities of coincident counts can be expressed in the form

$$P_{LR}^{(k,l)}(a,b)=\int d\lambda\,\rho(\lambda)P_A^{(k)}(\lambda,a)P_B^{(l)}(\lambda,b), \quad (48)$$

where $\rho(\lambda)$ is the distribution of the hidden variables, and $P_A^{(k)}(\lambda,a)$ is the probability of a detection of the photon at the kth detector behind the multiport A (see Fig. 7), if the local macroscopic parameters settings are at a, and the hidden variable describing the system is λ [6]. The probability $P_B^{(l)}(\lambda,b)$ is analogously defined for a detection event behind the multiport B. The locality assumption reveals itself by the absence of the parameter b in $P_A^{(k)}(\lambda,a)$, i.e., this probability is independent of the settings of the remote apparatus B, and analogously $P_B^{(k)}(\lambda,b)$ is independent of a. One immediately can derive the inequality (47) by recalling that that for any x, y, x' and y', which are between 0 and 1, one must have [45]

$$-1\leqslant xy+xy'+x'y-x'y'-x-y\leqslant 0, \quad (49)$$

putting $x=P_A^{(k)}(\lambda,a)$, $y=P_B^{(k)}(\lambda,b)$, etc., and finally averaging the resulting expression over the distribution $\rho(\lambda)$.

We shall now demonstrate that the Clauser-Horne inequalities are violated for any two Bell-multiport experiments. To make our reasoning as simple as possible let us restrict the range of the macroscopic parameters to those satisfying $\mathbf{\Phi}_{kl}^m=0$ for all $m\neq 1$ (i.e., we let only one local phase to be varied; the other ones are fixed at zero); then one obtains

$$P_{QM}^{(1,1)}(\phi_A^1,\phi_B^1)=\frac{1}{N^3}((N-1)^2+1+2(N-1)\cos(\phi_A^1+\phi_B^1)). \quad (50)$$

Putting this into the CH inequality we obtain (for the optimal settings) the contradiction

$$\frac{N-1}{N^3}(4\sqrt{2}-4)\leqslant 0. \quad (51)$$

Thus no local realistic description of the experiment is possible.

Let us now discuss the impact of some imperfections of the experiment on the above result. The visibility of the patterns followed by the probabilities in the actual experiment may be lower than the one predicted for the perfect case. We shall describe the expected form of the experimental results in the following way:

$$P_{\mathrm{expt}}^{(1,1)}(\phi_A^1+\phi_B^1)=(1-r)\frac{1}{N^2}+\frac{r}{N^3} \times((N-1)^2+1+2(N-1)\cos(\phi_A^1+\phi_B^1)), \quad (52)$$

where $0\leqslant r\leqslant 1$. The parameter r has been introduced to describe the reduction of the visibility of the underlying perfect quantum-interference pattern (50), due to various possible disturbances. The first term in Eq. (52) represents the ''noise'' introduced by these imperfections.

The threshold value for parameter r (above which we have a violation of CH inequality) is given by

$$r_{\mathrm{tr}}(N)=\frac{N}{N+(2\sqrt{2}-2)}. \quad (53)$$

For the lowest N's one has $r_{\mathrm{tr}}(2)=\sqrt{1/2}\approx 0.707$ (a well-known result), $r_{\mathrm{tr}}(3)\approx 0.784$, $r_{\mathrm{tr}}(4)\approx 0.826$, and $r_{\mathrm{tr}}(5)\approx 0.858$. This means, that the requirement on the perfection of the interferometric setup grows with N.

It is interesting to notice that the actual visibility of the modulation of the probability $P_{\mathrm{expt}}^{(1,1)}$ for the threshold r is given by

$$V_{\mathrm{tr}}(N)=\frac{2(N-1)(\sqrt{2}+1)}{2+(\sqrt{2}+1)((N-1)^2+1)}. \quad (54)$$

One now has $V_{\mathrm{tr}}(2)=\sqrt{1/2}\approx 70.7\%$, and surprisingly $V_{\mathrm{tr}}(3)\approx 68.6\%$, $V_{\mathrm{tr}}(4)\approx 55.4\%$, and $V_{\mathrm{tr}}(5)\approx 44.9\%$. This stems from the fact that for $N>2$ the visibility of the *perfect* quantum fringes, as predicted by Eq. (50) for $N>2$, is less than 100%, namely, $2(N-1)/[(N-1)^2+1]$.

Various imperfections of the experiment, like the approximate nature of the phase-matching condition (22), which may cause only one of the two entangled photons to pass the pinholes, losses at optical elements, and finally less than perfect quantum efficiency of the detectors, change the relative weight of the observed coincident counts to that of the singles. One can introduce a *collection efficiency parameter* η $(0<\eta<1)$ to describe the effect of all those imperfections (we tacitly assume a symmetric situation). The rate of counts at a single detector will be lowered by the factor η, i.e.,

$$P_{\mathrm{imperf}}^{(n)}=\eta P_{QM}^{(n)}, \quad (55)$$

where $n=k$ or l, whereas for the coincidences one will have

$$P_{\mathrm{imperf}}^{(k,l)}=\eta^2 P_{QM}^{(k,l)}. \quad (56)$$

Even for no visibility reduction, the threshold value of η allowing for a violation of the Bell inequality (47) is quite demanding, and reads

$$\eta_{\rm tr}(N)=\frac{N^2}{N^2+2(\sqrt{2}-1)(N-1)}, \tag{57}$$

i.e., one has $\eta_{\rm tr}(2)\approx 0.828$, $\eta_{\rm tr}(3)\approx 0.844$, and $\eta_{\rm tr}(4)\approx 0.865$.

If one allows all local phase settings to be varied in $P_{QM}^{(k,l)}$ [given by Eq. (35)], then one obtains a stronger violation of the Clauser-Horne inequality. For example, for the two tritter case, the search of the maximum of the middle expression of the CH inequality gives $\frac{2}{27}1.748>0$ (a MATHEMATICA calculation). This is slightly more than the value of the left-hand side of the expression (51) for $N=3$. Also the experimentally relevant parameters $r_{\rm tr}(3)$ and $\eta_{\rm tr}(3)$ decrease their values to 0.774 and 0.837, respectively. The second value is only slightly larger than the usual threshold for $N=2$.

We conjecture that future investigations will lead to different Bell inequalities, further lowering those limits. In the Appendix we present a version of the Bell theorem involving the correlation functions for which the critical value of r decreases to $\frac{3}{4}$.

VI. OPTICAL ANALOGS OF SPIN-1 STERN-GERLACH DEVICES AND THE KOCHEN-SPECKER CONTRADICTION

As was already mentioned earlier, thus far most of the theoretical studies of higher dimensional entanglement were confined to higher than $s=\frac{1}{2}$ correlated spins. There is a rich literature of the subject [45,28]. However, to our knowledge no experiment has been done.

We would like to present here an optical analog of the spin-1 EPR-Bell gedanken experiments. We are interested specifically in reproducing the experiment extensively discussed by Mermin and Schwarz, and other authors [40], which involved two spin-1 particles in a singlet state fed into two spatially separated Stern-Gerlach apparata.

A. Initial state

The beam entanglement shown in Fig. 6, clearly, can reproduce the properties of the singlet state of a two spin-1 system:

$$|\psi(3)\rangle=\sqrt{1/3}\sum_{m=-1}^{1}(-1)^m|m,A\rangle|-m,B\rangle, \tag{58}$$

where we have changed the numeration of the beams to make it correspond to the set of eigenvalues of spin-1. It is evident that the exact production of this state will be possible with appropriate tuning of all six phase shifts. However, in order to obtain state (58), up to a trivial external phase factor, it is enough to tune only two of them, say at side A (this is one of the striking properties of the entanglement).

B. Optical analog of a spin-1 Stern-Gerlach device

As the next step we construct a local measuring apparatus that would mimic the Stern-Gerlach device [47]. First of all, if the situation described by Eq. (58) is to be treated as equivalent to the spin case, then, due to the fact that the state of our photons represents an entanglement of the *directions* of propagation of the particles, measurement of the s_z component of the ''spin'' can be defined simply by placing, at each side of the experiment, three detectors (one for each beam). Thus if, say, the detector at side A in beam m clicks, such an event will be treated as equivalent to obtaining the value m in the case of a measurement of s_z performed upon a real spin-1 object.

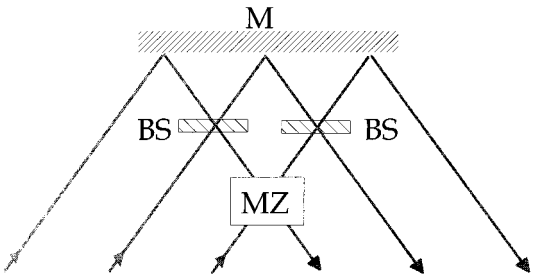

FIG. 11. The optical analog of a Stern-Gerlach device (simulation of a spin-1 particle). Only the devices needed to obtain the second, third, and fourth unitary transfomation of Eq. (61) are shown. The box represents a Mach-Zehnder (MZ) interferometer with a tunable internal phase θ, and the external phase correction [compare Eq. (62)]. The other two beam splitters are 50-50 ones, and the top object is a mirror. The unitary transformation (61), performed by the full device, acts upon a single-photon state, and is exactly equal (in the mathemacital sense) to the unitary transformation linking the spin-1 eigenstates of $\mathbf{s}\cdot\mathbf{z}$, where $\mathbf{z}=(0,0,1)$, with those of $\mathbf{s}\cdot\mathbf{n}$, where in turn $\mathbf{n}=(\sin\theta,\sin\theta,\cos\theta)$.

However, we must be also able to construct a device which is equivalent to measurement of an *arbitrary* component of spin-1. To this end, we need a multiport beam splitter which imparts on the local subsystem a unitary transformation which is identical to the one which transforms the eigenvectors of the z component of the spin, s_z, into the eigenstates of an arbitrary component $\mathbf{n}\cdot\mathbf{s}$. If the unit vector $\mathbf{n}$ is represented by

$$\mathbf{n}=(\sin\theta\cos\phi,\sin\theta\sin\phi,\cos\theta), \tag{59}$$

such a transformation can be represented (in the original basis) by the following product of unitary (rotation) matrices:

$$\begin{aligned}R(\mathbf{n})&=R_y(\theta)R_z(\phi)\\&=\begin{bmatrix}\frac{1}{2}(1+\cos\theta) & -\sqrt{\frac{1}{2}}\sin\theta & \frac{1}{2}(1-\cos\theta)\\ \sqrt{\frac{1}{2}}\sin\theta & \cos\theta & -\sqrt{\frac{1}{2}}\sin\theta\\ \frac{1}{2}(1-\cos\theta) & \sqrt{\frac{1}{2}}\sin\theta & \frac{1}{2}(1+\cos\theta)\end{bmatrix}\\&\times\begin{bmatrix}e^{-i\phi} & 0 & 0\\ 0 & 1 & 0\\ 0 & 0 & e^{i\phi}\end{bmatrix}.\end{aligned} \tag{60}$$

Of course, the diagonal matrix represents just two conjugate phase shifts performed upon the beams 1 and -1. The operational realization of the other matrix is more involved.

According to Reck *et al.* [35], any unitary operator can be split into a sequence of U(2) beam-splitter operators acting in

two-dimensional subspaces (this method includes also the possibility of relabelling of the output and input ports, and introducing phase shifts). Please note that one can decompose the matrix $\mathbf{R}_y(\theta)$ in the following way:

$$\begin{bmatrix} 0 & 1 & 0 \\ 1 & 0 & 0 \\ 0 & 0 & 1 \end{bmatrix} \begin{bmatrix} 1 & 0 & 0 \\ 0 & \sqrt{\frac{1}{2}} & \sqrt{\frac{1}{2}} \\ 0 & \sqrt{\frac{1}{2}} & -\sqrt{\frac{1}{2}} \end{bmatrix} \begin{bmatrix} \sin\theta & 0 & \cos\theta \\ 0 & 1 & 0 \\ \cos\theta & 0 & -\sin\theta \end{bmatrix}$$
$$\times \begin{bmatrix} -\sqrt{\frac{1}{2}} & \sqrt{\frac{1}{2}} & 0 \\ \sqrt{\frac{1}{2}} & \sqrt{\frac{1}{2}} & 0 \\ 0 & 0 & 1 \end{bmatrix} \begin{bmatrix} 0 & 0 & 1 \\ 1 & 0 & 0 \\ 0 & 1 & 0 \end{bmatrix}. \tag{61}$$

This decomposition defines the structure of the multiport device performing the transformation $R_y(\theta)$. The first and the last matrix represent trivial relabelings of the input and the output ports. The middle ones represent action of three standard 2×2 beam splitters, mixing, respectively, the amplitudes of first the beam 1 and 0, then 1 and -1, and finally 0 and -1. Thus, once one chooses a specific basis to represent the measurement of the spin component s_z, one can indeed construct a multiport of the properties specified by matrix (60). In this way one can select superpositions of the original photon basis states which are exact analogs of the eigenstates of the operator $\mathbf{n}\cdot\mathbf{s}$. In other words, a photon leaves the multiport via output port m with probability 1, only if its initial state was a coherent superposition of the original directions of propagation with coefficients exactly equal to the complex conjugate of the mth row of the matrix $R(\mathbf{n})$.

It is an interesting feature of the actual construction shown above that the angles ϕ and θ, which define the direction of the ''spin component,'' translate here in a simple way into the two opposite phase shifts [represented by $R_z(\phi)$], and the reflection and transmission amplitudes of only one beam splitter. If one wants the device to be tunable, so that, depending on the settings of the parameters, it would be able to perform *any* transformation $R(\mathbf{n})$, these amplitudes cannot be fixed. They must be variable. To this end, one can replace the middle beam splitter with an equivalent Mach-Zehnder interferometer (as shown in Fig. 11). One can build the Mach-Zehnder with the use of two symmetric beam splitters and two phase shifters. The unitary transformations representing these devices, when multiplied, should reproduce the matrix of the tunable beam splitter. For simplicity, we shall describe this property within the two-dimensional subspace of the degrees of freedom upon which the interferometer operates. An exemplary realization reads

$$\exp(i(\theta-\pi/2))\frac{1}{\sqrt{2}}\begin{bmatrix} 1 & i \\ i & 1 \end{bmatrix}\begin{bmatrix} e^{i2\theta} & 0 \\ 0 & 1 \end{bmatrix}\frac{1}{\sqrt{2}}\begin{bmatrix} 1 & i \\ i & 1 \end{bmatrix}$$
$$= \begin{bmatrix} \sin\theta & \cos\theta \\ \cos\theta & -\sin\theta \end{bmatrix}. \tag{62}$$

The overall phase shift, $\exp(i(\theta-\pi/2))$, is applied to compensate the relative phase otherwise introduced by such a device with respect to the third degree of freedom.

If one places three detectors behind the 3×3 multiport beam splitter performing the unitary transformation $R(\mathbf{n})$, one obtains an exact analog of a Stern-Gerlach device measuring the component $\mathbf{n}\cdot\mathbf{s}$ of the spin. With two such multiport devices, the state (58), and six detectors, one has all that is needed to perform the optical analog of the (usual) gedanken EPR-Bell experiments involving correlations of spin-1 particles.

Construction of devices like the ones described above is within the reach of any good quantum optical laboratory. It involves only standard optical elements. Thus the multiports open the possibility of actually performing the Bell-type (gedanken) experiments discussed in the literature. Since in the bibliography of the problem one can find the appropriate Bell inequalities for the experiment (e.g. [45]), we shall not discuss them here.

C. Optical analogs of the observables of the Kochen-Specker paradox

In this section we will present the construction of the optical analogs of the operators used in the reasoning of Kochen and Specker [26]. The paradoxical contradictions between realistic theories and quantum mechanics are in this case state independent. The properties of the operator algebra play the essential role. However, the postulates concerning realistic theories are of a different kind than those leading the Bell inequalities.

The argument assumes that for a realistic theory the (predetermined) results of measurements are independent of their context. That is, the result of the act of measurement of an operator, say $(\mathbf{s}\cdot\mathbf{n}_z)^2$ (where $\mathbf{n}_z$ is again a unit vector defining the z direction of a *certain* triad of orthogonal unit vectors), depends solely on the properties of the system to be measured. It should not depend on whether we measure $(\mathbf{s}\cdot\mathbf{n}_z)^2$ alone or *together* with *any* other commuting (i.e., commeasurable) observable. Kochen and Specker focused on operators like $(\mathbf{s}\cdot\mathbf{n}_z)^2$ because it has a degenerate spectrum. With such an operator one cannot unambiguously associate a complete set of commuting observables. There are many mutually noncommuting operators which still commute with $(\mathbf{s}\cdot\mathbf{n}_z)^2$. If an operator is degenerate, there are different bases in which it is diagonal. Such bases correspond, of course, to inequivalent operational situations.

An operator is called *maximal* if it possesses a nondegenerate spectrum. Thus its diagonalization is unambiguous. It refers to solely one operational procedure. For the spin-1 object one can easily find an example of a nontrivial maximal operator commuting with $(\mathbf{s}\cdot\mathbf{n}_z)^2$, namely

$$G(\mathbf{n}_x,\mathbf{n}_y,\mathbf{n}_z)=a(\mathbf{s}\cdot\mathbf{n}_x)^2+b(\mathbf{s}\cdot\mathbf{n}_y)^2+c(\mathbf{s}\cdot\mathbf{n}_z)^2 \tag{63}$$

(we do not denote this operator by its usual symbol, H [26], since it is a bit confusing, as this usually reserved in the literature for the Hamiltonian). The numbers a, b, and c are arbitrary distinct real numbers. Thanks to this fact the spectrum of G, which consists of $a+b$, $b+c$, and $c+a$, is nondegenerate.

One more crucial assumption of the Kochen-Specker discussion links the values of the outcomes of the measurements of commuting observables. Let the functional relation between the two observables, say A and B, be given by $B=f(A)$, where f is a certain function. A realistic theory would assign to each individual system, denoted here by the index k, of an ensemble described by the quantum state $|\psi\rangle$ a set of numerical values for each observable (A_k for A, B_k for B). These values must belong to the spectrum of the observables concerned. Thus one must have $B_k=f(A_k)$.

One has for any three orthogonal spatial directions $\mathbf{n}_x$, $\mathbf{n}_y$, and $\mathbf{n}_z$,

$$(\mathbf{s}\cdot\mathbf{n}_x)^2+(\mathbf{s}\cdot\mathbf{n}_y)^2+(\mathbf{s}\cdot\mathbf{n}_z)^2=s(s+1)=2. \tag{64}$$

Therefore, as the spectrum of each square of a component of the spin-1 operator consists solely of 0 and 1, one of the values $((s\cdot n_x)^2)_k$, $((s\cdot n_y)^2)_k$, and $((s\cdot n_z)^2)_k$ must be 0, and the other two 1.

The Kochen-Specker theorem shows that all that was said above is self-contradictory. A set of directions is given for which there is no possibility whatsoever to assign 1's and 0's in a way which is consistent with the constraint imposed by Eq. (64). For the detailed geometric argument leading to the above see [26,11,47].

The results of Sec. V enable us to propose optical analogs of the operational situations leading to the contradiction. We can already build a device reproducing any $\mathbf{s}\cdot\mathbf{n}_z$ operator. Obviously, the same device can be used to measure $(\mathbf{s}\cdot\mathbf{n}_z)^2$. We simply ignore the sign of the nonzero eigenvalue of $\mathbf{s}\cdot\mathbf{n}_z$. This sign may be even made totally inaccessible for us by superposing the beams $+1$ and -1 on a standard 50-50 beam splitter. Surprisingly, via this simple trick we create the operational procedure to measure $G(\mathbf{n}_x,\mathbf{n}_y,\mathbf{n}_z)$. It is easy to show that G has the following set of eigenvectors:

$$\begin{aligned}
|b+c\rangle &= \sqrt{\frac{1}{2}}(|-1\rangle_{\mathbf{n}_z}-|+1\rangle_{\mathbf{n}_z})=|0\rangle_{\mathbf{n}_x},\\
|a+c\rangle &= \sqrt{\frac{1}{2}}(|-1\rangle_{\mathbf{n}_z}+|+1\rangle_{\mathbf{n}_z})=|0\rangle_{\mathbf{n}_y},\\
|a+b\rangle &= |0\rangle_{\mathbf{n}_z},
\end{aligned} \tag{65}$$

where, e.g., $|0\rangle_{\mathbf{n}_z}$ denotes the eigenket of $\mathbf{s}\cdot\mathbf{n}_z$ associated with the eigenvalue 0. The beam splitter needed to perform this transformation is described by the matrix

$$\begin{bmatrix} -\sqrt{\frac{1}{2}} & 0 & \sqrt{\frac{1}{2}} \\ 0 & 1 & 0 \\ \sqrt{\frac{1}{2}} & 0 & \sqrt{\frac{1}{2}} \end{bmatrix}. \tag{66}$$

Further, as the argument rests upon different operational procedures which may pertain to the measurement of the same degenerate operator, we should be able to build $G(\mathbf{n}'_x,\mathbf{n}'_y,\mathbf{n}_z)$. This operator is similar in its nature to

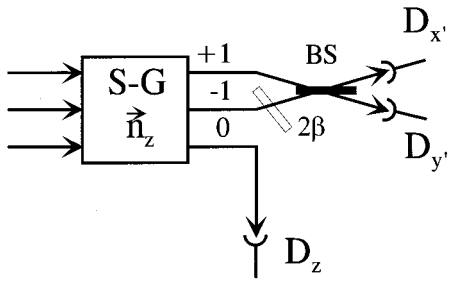

FIG. 12. The optical equivalent of the maximal observable G (for details see text). The device must discriminate between three eigenstates given by Eq. (68). This can be done by introducing a phase shift in the -1 beam of the value 2β. The beam splitter BS has a transformation matrix given by Eq. (66). The resulting output states differ from those of Eq. (68) only by overall phase factors. The system composed of the phase shifter and detector station $\{D_{x'},D_{y'}\}$ can be, in principle separated by an arbitraly long distance form the detector D_z (this enables one to invoke Einstein's locality in our argument).

$G(\mathbf{n}_x,\mathbf{n}_y,\mathbf{n}_z)$; however, a different triad of orthogonal directions is used. The z direction is still the same (this is required for the commeasurability of our G with $\mathbf{s}\cdot\mathbf{n}_z$), while the two other vectors have been rotated, say, by the angle β. It is obvious that the eigenstates of $G(\mathbf{n}'_x,\mathbf{n}'_y,\mathbf{n}_z)$ are given by:

$$\begin{aligned}
|b+c\rangle' &= \sqrt{\frac{1}{2}}(e^{i\beta}|-1\rangle_{\mathbf{n}_z}-e^{-i\beta}|+1\rangle_{\mathbf{n}_z})=|0\rangle_{\mathbf{n}'_x},\\
|a+c\rangle' &= \sqrt{\frac{1}{2}}(e^{i\beta}|-1\rangle_{\mathbf{n}_z}+e^{-i\beta}|+1\rangle_{\mathbf{n}_z})=|0\rangle_{\mathbf{n}'_y},
\end{aligned} \tag{67}$$

$$|a+b\rangle=|0\rangle_{\mathbf{n}_z}. \tag{68}$$

This can be achieved by introducing two opposite phase shifts behind the optical Stern-Gerlach device (a slightly modified version of this arrangement is presented in Fig. 12). The full transformation now reads

$$\begin{bmatrix} -\sqrt{\frac{1}{2}} & 0 & \sqrt{\frac{1}{2}} \\ 0 & 1 & 0 \\ \sqrt{\frac{1}{2}} & 0 & \sqrt{\frac{1}{2}} \end{bmatrix} \begin{bmatrix} e^{-i\beta} & 0 & 0 \\ 0 & 1 & 0 \\ 0 & 0 & e^{i\beta} \end{bmatrix}. \tag{69}$$

With the construction of this device we now have a method enabling us to build an optical equivalent of any of the operators involved in the Kochen-Specker reasoning.

The clear representation of the operational procedures involved in the Kochen-Specker argument enables one to understand more intuitively the physical reason for the contradiction. Let us imagine the following situation. We prepare a photon in an arbitrary state. It is important to make this preparation in an event-ready scheme [22]. This means that we use an operational procedure which enables us to know that we indeed have a single photon in the apparatus even before the actual detection (for details, see [22]). In this way we have a preparation of the system which fully agrees with

the quantum-mechanical interpretation of the state (i.e., as describing an ensemble of identically prepared systems). We pass the photon through the machine measuring $G(\mathbf{n}'_x,\mathbf{n}'_y,\mathbf{n}_z)$, in order to measure $(\mathbf{s}\cdot\mathbf{n}_z)^2$. Now, if we register a click at the detector D_z in the path 0, than we can say that the measured result is 0. No click in the path 0 means that the result is 1. Now, please note that the beam splitter, and the two conjugate phase shifters which define the other two directions involved, namely, $\mathbf{n}'_x,\mathbf{n}'_y$, can be placed arbitrarily far away from the aforementioned detector. Thus, Einstein's locality would demand that click or no click at D_z should not depend upon the setting of the remote phase β. This is a clear argument for noncontextuality in this case.

So where must the contextuality enter? The Kochen-and-Specker-type arguments ([25,26,11,46]) proceed by considering a whole series of orthogonal triads. If we want to build a tunable device which would provide optical analogs of maximal operators which are commeasurable with, say, $(\mathbf{s}\cdot\mathbf{n}_x)^2$, we can do it in the following way. First, we construct an optical Stern-Gerlach device for $(\mathbf{s}\cdot\mathbf{n}_x)$. Second, we build the $G(\mathbf{n}'_y,\mathbf{n}'_z,\mathbf{n}_x)$ device. The cyclic permutation of the indices x, y, and z has been done deliberately. Our construction of the operator defines first the unprimed vector, and behind this device we put the setup (69), which enables us to perform the rotation to the primed directions. The contextuality is transparent when one notices that the devices $G(\mathbf{n}_y,\mathbf{n}_z,\mathbf{n}_x)$ and $G(\mathbf{n}_x,\mathbf{n}_y,\mathbf{n}_z)$ are, from an operational point of view, different constructions. One cannot continuously modify the phase β to transform the first device into the second one. The two devices are interferometers of a completely different construction. Please note here the deep analogy with the version of the proof of the impossibility of noncontextual realistic models of quantum mechanics given by Bell [25].

The present authors view these facts as a direct manifestation of the validity of the operational ideas of Bohr, which are the main pillar of the Copenhagen interpretation.

VII. FINAL REMARKS

The present paper presents, *in statu nascendi*, the theory of some applications of the idea of optical multiport devices to areas of research connected with fundamental questions in quantum mechanics. One can expect experimental results to be presented soon ([32]). Also we expect new theoretical results, not necessarily of our authorship.

ACKNOWLEDGMENTS

The authors thank H. J. Bernstein and D. M. Greenberger for their contributions at the earlier stage of the project [30,35]. We also thank H. Weinfurter and M. Reck for many discussions. M.Z. acknowledges support of the University of Gdańsk Grants No. BW-5400-5-0062-5 and BW-5400-5-0087-6. Also, he thanks the coauthor (A.Z.) for his long-term collaboration and sponsoring (via the funds of the University of Innsbruck, and the 1996/97 Austrian-Polish scientific-technical collaboration Project No. 22). A.Z. and M.A.H. acknowledge support by the Austrian Fonds zur Förderung der Wissenschaftlichen Forschung (S65-02) and NSF Grant No. PHY92-13964. M.A.H. and M.Z. acknowledge the University of Innsbruck for hospitality.

APPENDIX: BELL THEOREM FOR THE TRITTER CORRELATION FUNCTION

The correlation functions described in the main text cannot be reproduced by any local realistic theory. We shall explicitly prove this claim here only for the two-tritter experiment (the generalization for higher Bell multiport beam splitters is possible).

Let us first write down the expected structure of a local hidden variable prediction for the two-tritter experiment. Motivated by simplicity, here we shall represent the local realistic theories by their version employing deterministic hidden variables. It is well known that, once the Bell theorem is established for this case, one can easily present its more refined versions [8].

We denote the set of hidden variables describing the individual system by λ, and the distribution of these for the ensemble of pairs of particles involved in the experiment by $\rho(\lambda)$. The result of the measurement at side $A(B)$, predetermined by λ, is given by functions $V_A(\phi_A^1,\phi_A^2,\phi_A^3;\lambda)$ $(V_B(\phi_B^1\phi_B^2\phi_B^3;\lambda))$. The functions V_A and V_B depend solely on the *local* settings of the phase shifters. The values of these functions are, of course, limited to the set of Bell numbers for the experiment, here α, α^2, and $\alpha^3=1$. We shall not assume any specific form of these functions. Following Bell [37], the local hidden variable prediction for the correlation function has the following structure:

$$E_{HV}(\phi_A^1,\phi_A^2,\phi_A^3;\phi_B^1,\phi_B^2,\phi_B^3) = \int d\lambda\,\rho(\lambda)V_A(\phi_A^1,\phi_A^2,\phi_A^3;\lambda)V_B(\phi_A^1,\phi_A^2,\phi_A^3;\lambda). \tag{A1}$$

Our aim is to show that the quantum prediction for the two-tritter experiment, namely [compare Eq. (45)]

$$E_{QM}(\phi_A^1,\phi_A^2,\phi_A^3;\phi_B^1,\phi_B^2,\phi_B^3) = \tfrac{1}{3}\sum_{m=1}^{3}\exp[i(\phi_A^m+\phi_B^m-\phi_A^{m+1}-\phi_B^{m+1})], \tag{A2}$$

where all indices are modulo 3, cannot be reproduced by (A1).

We shall present now a derivation of a simple Bell inequality for the two-tritter experiment [46], which will involve four local macroscopic parameter settings at each spatially separated location.

Thus we shall enable the experimenter at each side to choose between four possible settings of the system of local phase shifters. This is equivalent to testing the quantum correlation function E_{QM} at $4\times4=16$ points of its domain. Let us denote the four possible settings of the system of phase shifters in front of the tritter A by the index $a=1,\ldots,4$ (a similar index for the settings of the parameters at B will be called b). The phase shifts of the ath setting will be denoted by $\phi_A^{1(a)}$, $\phi_A^{2(a)}$, and $\phi_A^{3(a)}$ (similarly we have $\phi_B^{1(b)}$, $\phi_B^{2(b)}$, and $\phi_B^{3(b)}$ on side B). As it was mentioned earlier, one

can always choose the third phase to be 0 (this will be used below, and thus we skip this parameter from all expressions).

Let us first formulate a certain lemma. The matrix

$$N=\begin{bmatrix} 1 & \alpha^2 & 0 & \alpha \\ \alpha^2 & 1 & \alpha & 0 \\ 0 & \alpha & 1 & \alpha^2 \\ \alpha & 0 & \alpha^2 & 1 \end{bmatrix} \tag{A3}$$

has the following property:

$$\max\left|\sum_{a=1}^{4}\sum_{b=1}^{4}\alpha^{n_a+m_b}N^{ab}\right|=6, \tag{A4}$$

where the maximum is taken over all possible pairs of quadruples $\{n_1,n_2,\ n_3,\ n_4\}$ and $\{m_1,\ m_2,\ m_3,\ m_4\}$ of arbitrary natural numbers. Thus, the equality (A4) is a specific property of the Bell number α and the matrix N^{ab}. It is very easy to write a computer program to find the maximum.

Let us now apply this auxiliary lemma to our problem. The possible values of V_A and V_B are limited to the powers of α. Thus the upper bound of the expression

$$\max_{\lambda}\left|\sum_{a,b}V_A(\phi_A^{1(a)},\phi_A^{2(a)};\lambda)V_B(\phi_B^{1(b)},\phi_B^{2(b)};\lambda)N^{ab}\right| \tag{A5}$$

is 6. Please note, that this fact is independent of the actual phases defining V_A and V_B.

The hidden variable correlation function has the structure (A1). The modulus of an average of a variable cannot be greater than the maximum modulus of its value. Thus, after averaging the expression (A5) over $\rho(\lambda)$, we finally obtain a *Bell inequality* for the problem in the form of upper bound for the sum of the products of the values of the hidden variable correlation function. The explicit form of the inequality reads

$$\left|\sum_{a,b}E_{HV}(\phi_A^{1(a)},\phi_A^{2(a)};\phi_B^{1(b)},\phi_B^{2(b)})N^{ab}\right|\leqslant 6, \tag{A6}$$

The quantum predictions can violate this inequality. If, for the phases on side A, one chooses the settings

$$\{\phi_A^{1(1)},\phi_A^{1(2)},\phi_A^{1(3)},\phi_A^{1(4)}\}=\{\pi/3,4\pi/3,4\pi/3,\pi/3\}, \tag{A7}$$

$$\{\phi_A^{2(1)},\phi_A^{2(2)},\phi_A^{2(3)},\phi_A^{2(4)}\}=\{\pi/3,\pi/3,4\pi/3,4\pi/3\}, \tag{A8}$$

and, for side B,

$$\{\phi_B^{1(1)},\phi_B^{1(2)},\phi_B^{1(3)},\phi_B^{1(4)}\}=\{0,\pi,\pi,0\}, \tag{A9}$$

$$\{\phi_B^{2(1)},\phi_B^{2(2)},\phi_B^{2(3)},\phi_B^{2(4)}\}=\{0,0,\pi,\pi\}, \tag{A10}$$

then for the chosen phases the quantum prediction satisfies

$$E_{QM}^{ab}\equiv E_{QM}(\phi_A^{1(a)},\phi_A^{2(a)};\phi_B^{1(b)},\phi_B^{2(b)})=\frac{2}{3}N^{ab}*, \tag{A11}$$

where * denotes complex conjugation.

It is very easy to check that at the specific settings, namely, Eqs. (A7)–(A10), the quantum predictions, when inserted to inequality (A6) instead of E_{HV}, violate this inequality, as evidently

$$\sum_{a,b}E_{QM}^{ab}N^{ab}=\tfrac{2}{3}\sum_{a,b}N^{ab}*N^{ab}=8, \tag{A12}$$

thus we have a violation of the Bell inequality Eq. (A6) by $33\frac{1}{3}\%$.

In the actual experiment one cannot expect that the probabilities will follow the pattern given by Eq. (27), but rather the data would be close to the following:

$$\begin{aligned}P_{QM}^{\text{expt}}(k,n)=(1/3)^3\{3+r[&2\cos(\phi_A^1+\phi_B^1-\phi_A^2-\phi_B^2-\Phi^{kn})\\&+\cos(\phi_A^2+\phi_B^2-\phi_A^3-\phi_B^3-\Phi^{kn})\\&+\cos(\phi_A^3+\phi_B^3-\phi_A^1+\phi_B^1-\Phi^{kn})]\},\end{aligned} \tag{A13}$$

i.e., we expect to observe, due to various reasons, lower visibility (given by r) than 1. Due to the above, the experimental correlation function, E_{expt}, would also have its variations degraded by the same factor:

$$\begin{aligned}&E_{\text{expt}}(\phi_A^{1(a)},\phi_A^{2(a)};\phi_B^{1(b)},\phi_B^{2(b)})\\&\quad=rE_{QM}(\phi_A^{1(a)},\phi_A^{2(a)};\phi_B^{1(b)},\phi_B^{2(b)}).\end{aligned} \tag{A14}$$

We can insert E_{expt} into Eq. (A6), instead of E_{HV}, and fix its settings to the phases defining Eq. (A11), thus obtaining

$$\sum_{a,b}E_{\text{expt}}^{ab}N^{ab}=8r. \tag{A15}$$

It is clear that the inequality (A6) is violated only for $r>\frac{3}{4}$. This is a considerable improvement over the Clauser-Horne inequalities studied in the main text.

[1] E. Schrödinger, Naturwissenschaften **23**, 807 (1935); **23**, 823 (1935); **23**, 844 (1935).

[2] A. Aspect, P. Dalibard, and G. Roger, Phys. Rev. Lett. **49**, 1804 (1982).

[3] S. J. Freedman and J. F. Clauser, Phys. Rev. Lett. **28**, 938 (1972).

[4] P. R. Tapster, J. G. Rarity, and P. C. M. Owens, Phys. Rev. Lett. **73**, 1923 (1994).

[5] E. Santos, Phys. Rev. A **46**, 3646 (1992).

[6] J. F. Clauser and A. Shimony, Rep. Prog. Phys. **41**, 1881 (1978).

[7] L. E. Ballentine, Am. J. Phys. **55**, 785 (1987).

[8] D. M. Greenberger, M. Horne, A. Shimony, and A. Zeilinger, Am. J. Phys. **58**, 1131 (1990).

[9] D. Home and F. Selleri, Riv. Nuovo Cimento, **14**, 1 (1991).

[10] A. V. Belinskii and D. N. Klyshko, Laser Phys. **2**, 112 (1992);

Usp. Fiz. Nauk **163**, 1 (1993) Sov. Phys. Usp. **36**, 653 (1993)].
[11] A. Peres, *Quantum Theory: Concepts and Methods* (Kluwer, Dordrecht, 1993).
[12] M. A. Horne and A. Zeilinger, in *Symposium on Foundations of Modern Physics*, edited by P. Lahti and P. Mittelstaedt (World Scientific, Singapore, 1985); for first feasible proposal, see M. Zukowski and J. Pykacz, Phys. Lett. A **127**, 1 (1988).
[13] M. A. Horne, A. Shimony, and A. Zeilinger, Phys. Rev. Lett. **62**, 2209 (1989).
[14] Z. Y. Ou and L. Mandel, Phys. Rev. Lett. **61**, 50 (1988).
[15] S. Haroche, Ann. N. Y. Acad. Sci. **755**, 73 (1995).
[16] K. Wódkiewicz, Liwei Wang, and J. H. Eberly, Phys. Rev. A **47**, 3280 (1993).
[17] A. K. Ekert, Phys. Rev. Lett. **67**, 661 (1991).
[18] C. H. Bennett, G. Brassard, C. Crepeau, D. Jozsa, A. Peres, and W. K. Wootters, Phys. Rev. Lett. **70,** 1895 (1993).
[19] C. H. Bennett and S. J. Wiesner, Phys. Rev. Lett. **69**, 2881 (1992).
[20] A. M. Steinberg, P. G. Kwiat, and R. Chiao, Phys. Rev. Lett. **71**, 708 (1993).
[21] C. K. Hong, Z. Y. Ou, and L. Mandel, Phys. Rev. Lett. **59**, 2044 (1987).
[22] B. Yurke and D. Stoler, Phys. Rev. Lett. **68**, 1251 (1992); M. Żukowski, A. Zeilinger, M. A. Horne, and A. K. Ekert, *ibid.* **71**, 4287 (1993).
[23] M. Żukowski, A. Zeilinger, and H. Weinfurter, Ann. N. Y. Acad. Sci. **755**, 91 (1995).
[24] A. M. Gleason, J. Math. Mech. **6**, 885 (1957).
[25] J. S. Bell, Rev. Mod. Phys. **38**, 447 (1966).
[26] S. Kochen and E. Specker, J. Math. Mech. **17**, 59 (1967).
[27] P. Heywood and M. G. Redhead, Found. Phys. **13**, 481 (1983); see also H. R. Brown and G. Svetlichny, *ibid.* **20**, 1379 (1990).
[28] K. Wódkiewicz, in *Santa Fe Workshop of Foundations of Quantum Mechanics*, edited by T. D. Black *et al.* (World Scientific, Singapore 1992), p. 276; Acta Phys. Pol. **86**, 223 (1994); Phys. Rev A **51**, 2785 (1995).
[29] Note that photons have a zero rest mass, and thus their polarization variables have the properties of spin $\frac{1}{2}$.
[30] A. Zeilinger, H. J. Bernstein, D. M. Greenberger, M. A. Horne, and M. Zukowski, in *Quantum Control and Measurement*, edited by H. Ezawa and Y. Murayama (Elsevier, Amsterdam, 1993); A. Zeilinger, M. Żukowski, M. A. Horne, H. J. Bernstein, and D. M. Greenberger, in *Quantum Interferometry*, edited by F. DeMartini and A. Zeilinger (World Scientific, Singapore, 1994).
[31] C. Mattle, M. Michler, H. Weinfurter, A. Zeilinger, and M. Żukowski, Appl. Phys. B **60**, S111 (1995); G. Weihs, M. Reck, H. Weinfurter, and A. Zeilinger, Opt. Lett. **21**, 302 (1996).
[32] M. Reck, Ph.D. thesis University of Innsbruck, 1996 (unpublished).
[33] N. G. Walker and J. E. Carroll, Opt. Quantum Electron. **18**, 355 (1986); N. G. Walker, J. Mod. Opt. **34**, 15 (1987).
[34] D. N. Klyshko, Phys. Lett. A **132**, 299 (1988).
[35] M. Reck, A. Zeilinger, H. J. Bernstein, and P. Bertani, Phys. Rev. Lett. **73**, 58 (1994).
[36] D. Bohm, *Quantum Theory* (Prentice-Hall, Englewood Cliffs, NJ, 1951).
[37] J. S. Bell, Physics **1**, 195 (1965).
[38] J. G. Rarity and P. R. Tapster, Phys. Rev. Lett. **64**, 2495 (1990).
[39] H. J. Bernstein, J. Math. Phys. **15**, 1677 (1974).
[40] I. Jex, S. Stenholm, and A. Zeilinger, Opt. Commun. **117**, 95 (1995); P. Törma, S. Stenholm, and I. Jex, Phys. Rev. A **54**, 943 (1996); R. F. Werner (unpublished).
[41] I. D. Ivanovic, J. Phys. A **14**, 3241 (1981); W. K. Wooters, Found. Phys. **16**, 391 (1986); J. Schwinger, Proc. Natl. Acad. Sci. U.S.A. **46**, 570 (1960).
[42] B. R. Mollow, Phys. Rev. A **8**, 2684 (1973).
[43] C. K. Hong and L. Mandel, Phys. Rev. A **31**, 2409 (1985).
[44] J. F. Clauser and M. A. Horne, Phys. Rev. D **10**, 526 (1974).
[45] N. D. Mermin, Phys. Rev. D **22**, 356 (1980); A. Garg and N. D. Mermin, Phys. Rev Lett. **49**, 901 (1982); N. D. Mermin and G. M. Schwarz, Found. Phys. **12**, 101 (1982); M. Ardehali, Phys. Rev. D **44**, 3336 (1991); G. S. Agarwal, Phys. Rev. A **47**, 4608 (1993); K. Wódkiewicz, Acta Phys. Pol. **86**, 223 (1994).
[46] A different version of the discussion concerning optical analogs of spin-1 measurements has been presented in C. Ulrich, Diplomathesis, Technical University Vienna, 1993 (in German, unpublished).
[47] N. D. Mermin, Rev. Mod. Phys. **65**, 803 (1993).
[48] M. Żukowski, Laser Phys. **4**, 690 (1994).